REGULAR ARTICLE

blood advances

Bone marrow stroma cells promote induction of a chemoresistant and prognostic unfavorable S100A8/A9^{high} AML cell subset

Martin Böttcher,[1,2,*] Konstantinos Panagiotidis,[1,*] Heiko Bruns,[1] Martina Stumpf,[1] Simon Völkl,[1] Stefanie Geyh,[3] Barbara Dietel,[4] Thomas Schroeder,[3,5] Andreas Mackensen,[1,6] and Dimitrios Mougiakakos[1,2,6]

[1]Department of Internal Medicine 5 for Hematology and Oncology, Friedrich-Alexander-Universität, Erlangen-Nürnberg, Germany; [2]Department of Hematology and Oncology, University Hospital, Otto-von-Guericke University, Magdeburg, Germany; [3]Department of Hematology, Oncology, and Clinical Immunology, Medical Faculty, University of Düsseldorf, Düsseldorf Germany; [4]Department of Medicine 2 for Cardiology and Angiology, Friedrich-Alexander-Universität, Erlangen-Nürnberg, Germany; [5]Department of Hematology and Stem Cell Transplantation, University Hospital Essen, University Duisburg-Essen, Essen, Germany; and [6]Deutsches Zentrum Immuntherapie (DZI), Erlangen, Germany

Key Points

- Stroma cells promote induction of an S100A8/A9^{high} AML cell subset via IL-6/Jak/STAT3 signaling.
- S100A8/A9^{high} AML cells display a distinct metabolic, differentiation, and chemoresistance profile.

The bone marrow (BM) stroma represents a protective niche for acute myeloid leukemia (AML) cells. However, the complex underlying mechanisms remain to be fully elucidated. We found 2 small, intracellular, calcium-sensing molecules, S100A8 and S100A9, among the top genes being upregulated in primary AML blasts upon stromal contact. As members of the S100 protein family, they can modulate such cellular processes as proliferation, migration, and differentiation. Dysregulation of S100 proteins is described as a predictor of poor survival in different human cancers, including increased S100A8 expression in *de novo* AML. Thus, we wanted to decipher the underlying pathways of stroma-mediated S100A8/A9 induction, as well as its functional consequences. Upregulation of S100A8/A9 after stromal cross talk was validated in AML cell lines, was contact independent and reversible and resulted in accumulation of S100A8/A9^{high} cells. Accordingly, frequency of S100A8/A9^{high} AML blasts was higher in the patients' BM than in peripheral blood. The S100A8/A9^{high} AML cell population displayed enhanced utilization of free fatty acids, features of a more mature myeloid phenotype, and increased resilience toward chemotherapeutics and BCL2 inhibition. We identified stromal cell–derived interleukin-6 (IL-6) as the trigger for a Jak/STAT3 signaling-mediated S100A8/A9 induction. Interfering with fatty acid uptake and the IL-6-Jak/STAT3 pathway antagonized formation of S100A8/A9^{high} cells and therapeutic resistance, which could have therapeutic implications as a strategy to interfere with the AML-niche dynamics.

Introduction

Acute myeloid leukemia (AML) is a malignant disorder characterized by clonal expansion of immature myeloblasts that initially accumulate in the bone marrow (BM) and eventually in the peripheral blood (PB).[1] The incidence increases with age, with the median age of diagnosis being 67 years.[2] Cytogenetic and molecular abnormalities determine disease prognosis. Current therapeutic strategies include chemotherapy (particularly cytarabine in combination with anthracycline); targeted approaches, such as FLT3 or BCL2 inhibitors, epigenetic modifiers, and CD33-directed immunotoxins; and allogeneic

Submitted 12 August 2021; accepted 20 March 2022; prepublished online on *Blood Advances* First Edition 7 April 2022; final version published online 31 October 2022. https://doi.org/10.1182/bloodadvances.2021005938.

*M.B. and K.P. contributed equally to this study.

For original data, please contact dimitrios.mougiakakos@uk-erlangen.de.

The full-text version of this article contains a data supplement.

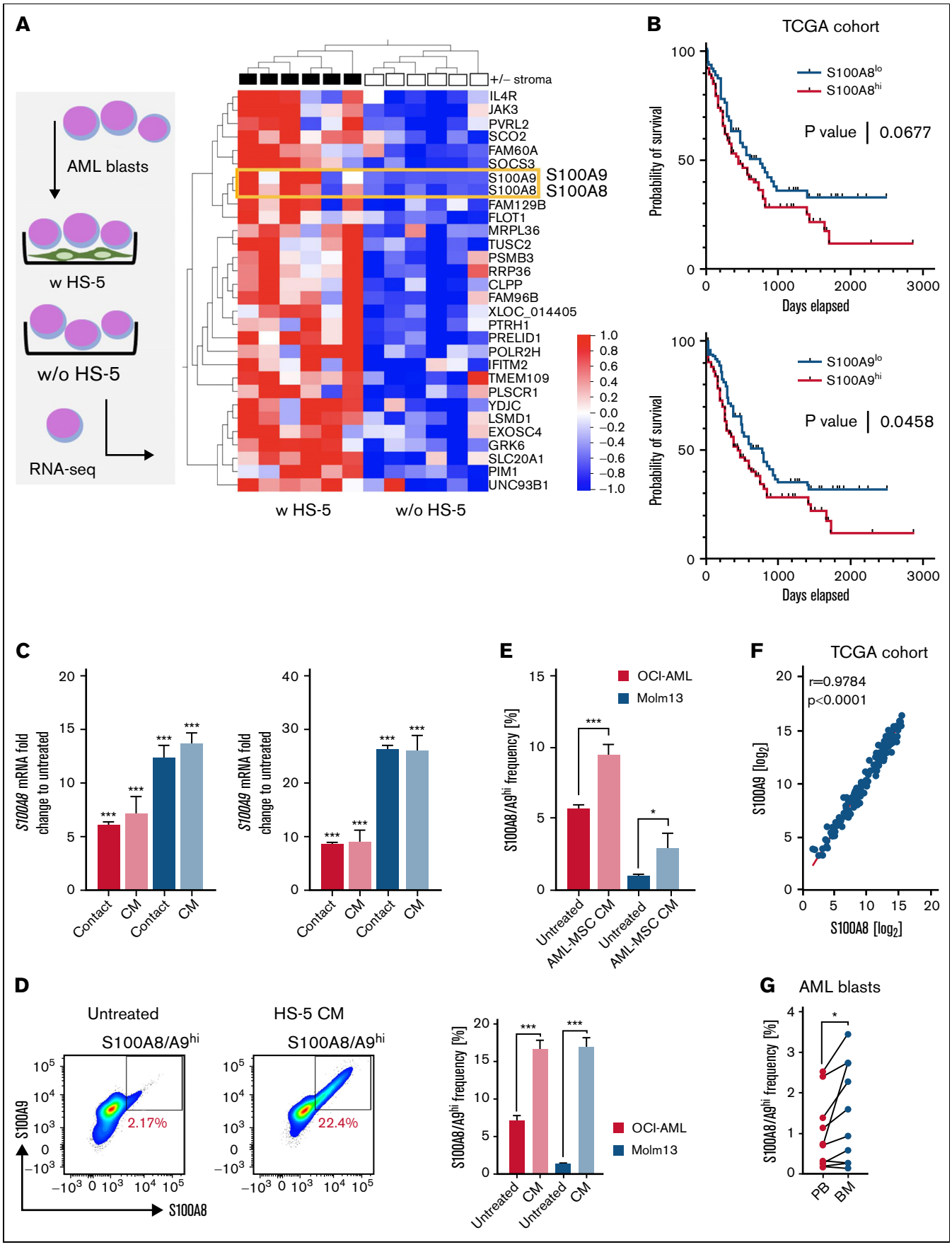

Figure 1.

hematopoietic stem cell (HSC) transplantation. Despite the improvement in diagnosing and treating AML, the 5-year overall survival rate is only 25% to 30% because of relapse, refractory disease, and disease-related mortality. Therefore, improving treatment outcome remains a high unmet need for most patients with AML.

In line with the "niche" concept, AML blasts closely interact with the stromal component of the BM microenvironment, similar to their nonmalignant counterparts.[3] Emerging evidence suggests that BM-derived mesenchymal stromal cells (BM-MSCs) support leukemia cell survival and confer chemoprotection. The underlying mechanisms of stromal-mediated protection of AML blasts is complex. Contact with BM-MSCs promotes proliferation, activates detoxifying ATP-binding cassette transporters, leads to enhanced antioxidative properties, and skews metabolism toward oxidative phosphorylation.[4,5] In this way BM-MSCs protect AML blasts from spontaneous and drug-induced cell death.[6] BM-MSC–derived factors that trigger those phenomena include, among others, free fatty acids[7]; chemokines, such as CXCL-8[8] and CXCL-12[9]; mitochondrial transfer[10]; and the adhesion molecule CD44.[11] In fact, cross talk between BM-MSCs and AML blasts is bidirectional, as malignant cells can remodel their BM niche to suppress regular hematopoiesis.[12] Consequently, BM is considered the primary site for minimal residual disease that gives rise to AML relapse and is a critical mediator of drug resistance. Therefore, a better understanding of the pathophysiological processes within the BM niche is inevitable for identifying novel therapeutic targets to improve treatment efficacy.

In addition to the aforementioned genetic features, high S100A8/A9 levels in AML blasts can be of negative prognostic impact.[13-15] Because of the higher stability, S100A8/A9 heterodimers, also known as calprotectin, are more abundant than the respective homodimers. S100A8/A9 belong to the S100 protein family, which comprises 20 members and is found only in vertebrates.[16] They possess a high number of functional targets and are therefore involved in different cellular processes including proliferation, differentiation, inflammation, Ca^{2+} homeostasis, apoptosis, and migration. When secreted, S100 proteins interact with several receptors, such as the fatty acid transporter CD36,[17] Toll-like receptor 4 (TLR4),[18] and the receptor for advanced glycation end products (RAGE).[19] S100A8 mainly signals via RAGE and S100A9 via TLR4. Dysregulation of S100 proteins (including their upregulation) is regularly reported in malignant entities.[16] S100A8 has been linked to leukemogenesis, because it maintains cells in an undifferentiated state during myelopoiesis.[18] In fact, S100A8 gene expression is elevated in the BM of patients with newly diagnosed or freshly relapsed AML and is associated with drug resistance (to conventional chemotherapy and novel agents, such as FLT3 or BCL2 inhibitors).[14,20] An increased S100A9-to-S100A8 ratio (by at least 10-fold) has been associated with myeloid differentiation in AML.[18,21] Coexpression of S100A8/A9 is upregulated during AML progression and correlates with the transition of AML blasts from the BM to the PB.[18] Accordingly, S100A8/A9 messenger RNA (mRNA) levels are increased in patients with AML with a higher circulating leukemic burden.[22]

Although S100A8/A9 expression in BM-MSCs correlates with the risk of preleukemic myelodysplastic syndrome transforming into AML,[23] it is unknown whether stromal cells affect S100A8/A9 expression. We report that MSCs promote induction of an S100A8/A9^{high} AML subset with distinct metabolic characteristics, features of a differentiated phenotype, and an increased resistance toward chemotherapeutics and BCL2 inhibitors. We identified the interleukin-6 (IL-6)/Jak/STAT3 signaling axis as the underlying molecular pathway, which we pharmacologically targeted and which could have therapeutic implications as a strategy to interfere with the AML niche dynamics.

Methods

Patient samples and cell lines

PB and BM samples from patients with AML were obtained upon receipt of their informed consent and in accordance with the Declaration of Helsinki (Ethics Committee approval 219_14B). Mononuclear cells from the PB or BM were obtained with Ficoll-Paque (GE Healthcare, Chicago, IL). Patient characteristics can be found in supplemental Table 1. MSCs were isolated from iliac crest BM aspirates taken from patients with newly diagnosed AML (Ethics Committee Approval 4777) by density gradient centrifugation and were expanded as previously detailed, while fulfilling uniformly minimal criteria.[24]

The human BM stroma cell line HS-5 was purchased from ATCC (Manassas, VA). The AML cell lines OCI-AML3 and MOLM-13 were purchased from DSMZ (Braunschweig, Germany). *Mycoplasma* contamination was regularly assessed with the Venor GeM Classic *Mycoplasma* detection kit (Minerva Biolabs, Berlin, Germany), according to the manufacturer's instructions, and authentication of the cell lines was performed.

Figure 1. BM stromal cells induce S100A8 and S100A9 in AML cells. (A) FACS-sorted primary CD33^{+}CD34^{+} AML blasts (n = 6) were cultured for 24 hours in the absence (w/o) or presence (w) of a confluent layer of the human BM-derived stroma cell line HS-5 and subsequently analyzed by microarray analysis (left). The heat map (right) shows the top 30 highest differentially expressed genes in the group of AML blasts cultured in the presence of HS-5 cells. (B) Publicly available data from TCGA (LAML data set) was divided into S100A8^{hi}/S100A9^{hi} and S100A8^{lo}/S100A9^{lo} groups based on the mean expression, and depicted as survival curves using the Mantel-Cox test for calculation of significance. (C) AML cell lines OCI-AML3 and MOLM-13 were cultured for 48 hours in the presence or absence of HS-5 cells (contact; OCI-AML, n = 11; MOLM-13, n = 10) or HS-5 CM (CM; OCI-AML, n = 5; MOLM-13, n = 5). Gene expression of *S100A8* and *S100A9* was analyzed by qPCR and is depicted as the fold change of treated/untreated cells (untreated set as 1). (D) Frequency of S100A8/S100A9^{hi} cells as shown in the representative pseudocolored flow cytometry plot was determined in AML cell lines (OCI-AML, n = 27; MOLM-13, n = 27) cultured for 48 hours in the absence or presence of HS-5 CM. (E) AML cell lines (OCI-AML, n = 13; MOLM-13, n = 11) were cultured for 48 hours in the absence or presence of CM from MSCs of 7 patients with AML (AML-MSC CM, patient ID 11-17; supplemental Table 1) and analyzed for the frequency of the S100A8/A9^{hi} population by flow cytometry. (F) Log_2-transformed normalized counts of the *S100A8* and *S100A9* gene expression (from the TCGA LAML data set) were correlated by the Spearman test. (G) The S100A8/A9^{hi} population among matched-pair PB- and BM-derived AML blasts (n = 10; patient ID 1-10; supplemental Table 1) was analyzed by flow cytometry. Data are expressed as the standard error of mean. *$P < .05$; **$P < .01$; ***$P < .001$. FACS, fluorescence-activated cell sorting; qPCR, quantitative real-time polymerase chain reaction.

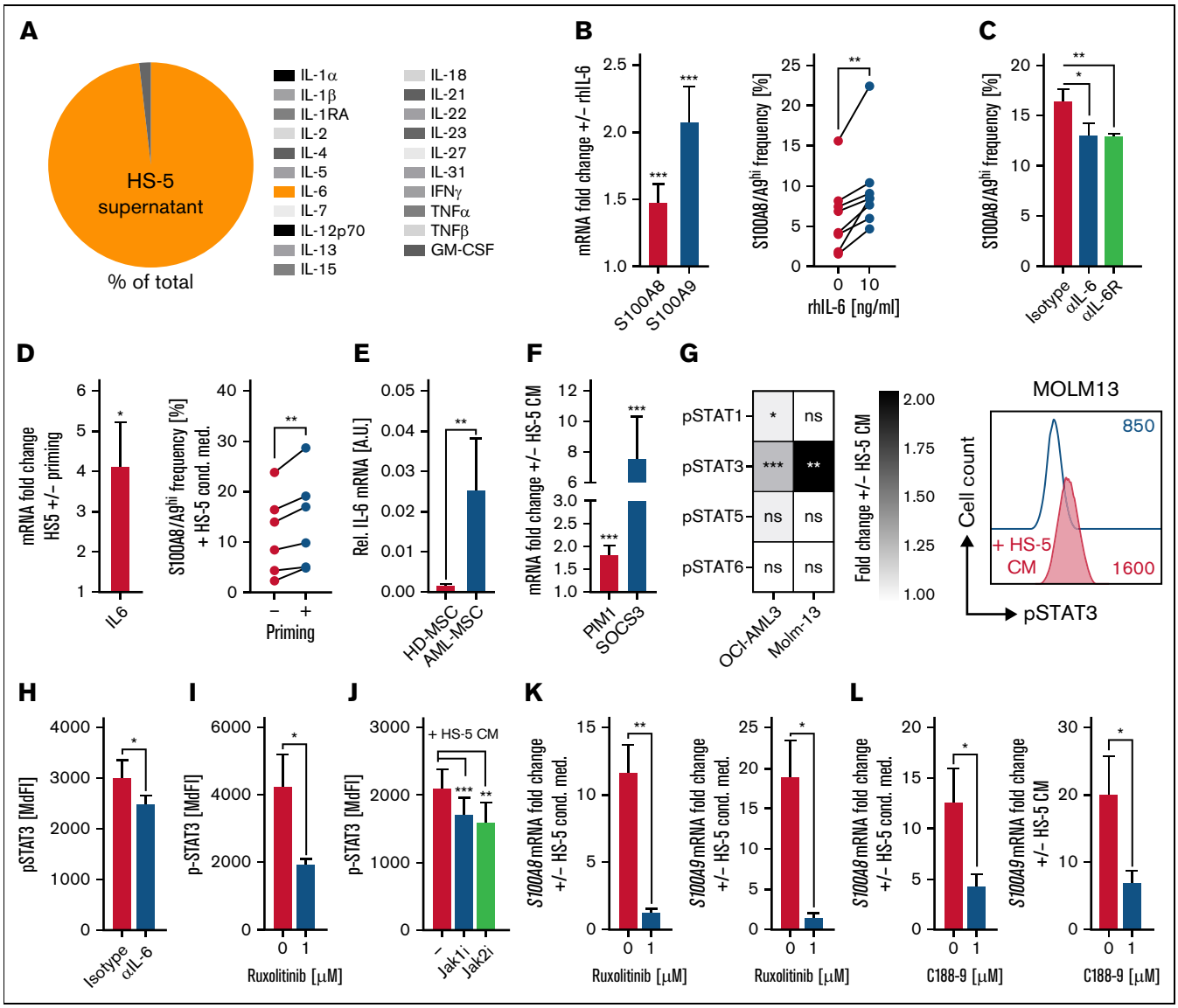

Figure 2. S100A8 and S100A9 is induced via IL-6/Jak/STAT3 signaling. (A) CM from HS-5 cells (n = 8) was analyzed with a bead-based multiplex assay for 25 human cytokines (IL-9, IL-10, IL-17A, and interferon α [IFN-α] not detected). The pie chart displays the individual proportion among the total analytes. (B) Induction of S100A8 and S100A9 on the mRNA (left; OCI, n = 4; MOLM-13, n = 5) and induction of an S100A8/A9^{hi} population (right; OCI-AML, n = 4; MOLM-13, n = 4) were analyzed after treatment with 10 ng/mL of rhIL-6 for 48 hours by qPCR and flow cytometry, respectively. mRNA levels are shown as the fold change with or without rhIL-6 (untreated set as 1). (C) Frequency of S100A8/A9^{hi} AML cells was determined by flow cytometry after culturing HS-5 CM-treated MOLM-13 cells (n = 4) in the absence (isotype) or presence of 10 μg/mL anti-IL-6 or anti-IL-6R blocking antibodies. (D) CM from HS-5 cells was prepared after inflammatory priming of the HS-5 cells (with 15 ng/mL tumor necrosis factor-α and 10 ng/mL IFN-γ). Gene expression of IL-6 in HS-5 cells was determined by qPCR and expressed as fold change between primed and nonprimed samples (nonprimed samples set as 1; left, n = 4). The frequency of S100A8/A9^{hi} AML cells (right; OCI-AML, n = 2; MOLM-13, n = 4) cultured with nonprimed and primed HS-5 CM for 48 hours was determined by intracellular flow cytometry. (E) Gene expression of *IL-6* was determined in healthy donor– and AML patient–derived BM-MSCs (both n = 5). (F) Gene expression of *PIM1* and *SOCS3* (2 STAT3 target genes) was determined in AML cell lines (OCI-AML n = 3, MOLM-13 n = 3) cultured in the absence or presence of HS-5 CM for 48 hours by qPCR and is shown as the fold change (untreated set as 1). (G) Phosphorylation of the STAT proteins (p-STAT) 1, 3, 5, and 6 was determined by PhosFlow in AML cell lines (OCI-AML, n = 3; MOLM-13, n = 3) cultured in the absence or presence of HS-5 CM for 20 minutes and is depicted as a heat map showing the fold change with or without HS-5 CM (left; untreated set as 1). Most prominently, p-STAT3 was induced by HS-5 CM treatment as representatively shown in the histogram (right; scale indicates median fluorescence intensity). (H-J) STAT3 phosphorylation was analyzed by PhosFlow in AML cell lines cultured in the presence of HS-5 CM for 20 minutes after pretreatment for 2 hours with anti-IL-6–blocking antibodies (H; OCI-AML, n = 3; MOLM-13, n = 3), ruxolitinib (I; OCI-AML, n = 2; MOLM-13, n = 2), and Jak1 or Jak2 inhibitor (J; OCI-AML, n = 2; MOLM-13, n = 2). (K-L) Induction of *S100A8* and *S100A9* gene expression after 48 hours of culture with HS-5 CM was analyzed in the absence (0 μM) or presence (1 μM) of the pan-Jak inhibitor ruxolitinib (K; OCI-AML, n = 3; MOLM-13, n = 3) or the p-STAT3 inhibitor C188-9 (L; OCI-AML, n = 5; MOLM-13, n = 5). Values are depicted as fold change with or without HS-5 CM (untreated set as 1). Data are expressed as the standard error of mean. *$P < .05$; **$P < .01$; ***$P < .001$; ns, not significant. qPCR, quantitative real-time polymerase chain reaction.

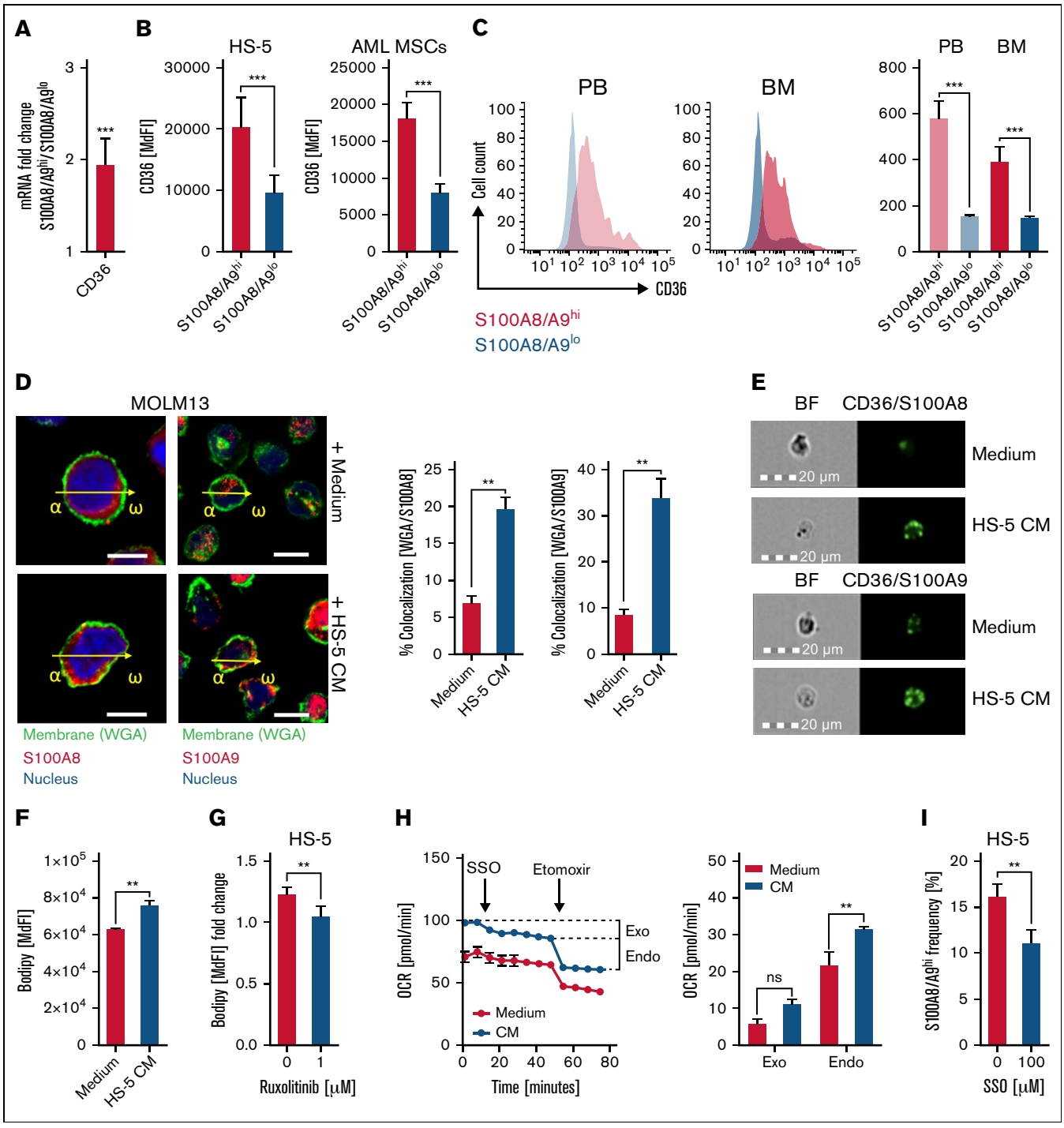

Figure 3. S100A8/A9^{hi} AML cells display enhanced fatty acid metabolism. (A) Gene expression of the fatty acid translocase *CD36* was determined in FACS-sorted S100A8/A9^{hi} and S100A8/A9^{lo} OCI-AML (n = 3) and MOLM-13 (n = 3) cells cultured for 48 hours in the presence of HS-5 CM by qPCR and is shown as the fold change (S100A8/A9^{lo} cells were set as 1). (B) Surface levels of CD36 were determined by flow cytometry on S100A8/A9^{hi} and S100A8/A9^{lo} cells among the AML cell lines cultured for 48 hours in the presence of CM from either HS-5 cells (left; OCI-AML, n = 4; MOLM-13, n = 4) or AML-MSCs isolated from 6 patients (right; OCI-AML, n = 12; MOLM-13, n = 12, patient ID 11-16; supplemental Table 1). (C) Surface levels of CD36 were analyzed by flow cytometry in matched-pair (n = 10; patient ID 1-10; supplemental Table 1) PB- and BM-derived S100A8/A9^{hi} and S100A8/A9^{lo} AML blasts, as representatively shown in histograms (left) and summarized in a bar graph (right). (D) Localization of S100A8 and S100A9 was visualized by fluorescence microscopy (left, scale bars = 20 µm). MOLM-13 cells (n = 5) were cultured in the absence (top) or presence (bottom) of HS-5 CM and stained for the cell membrane (WGA, green), S100A8 (left, red) or S100A9 (right, red), and the nucleus (blue, DAPI). Co-localization of S100A8/S100A9 and WGA were calculated with ZEN software (bar graphs; Zeiss). (E) A proximity ligation was performed with a Duolink Flow kit (Sigma-Aldrich) with antibodies against S100A8, S100A9, and CD36. The representative images show the bright-field (left, BF) and the fluorescence signal (right) in MOLM-13 cells. Bars represent 20 µm for 20× magnification.

Cell culture

For coculture experiments, HS-5 cells were seeded 24 hours before the addition of AML cells. Either 5×10^6 primary, sorted $CD45^+CD33^+CD34^+$ AML blasts were added to 5×10^4 HS-5 cells, or 2×10^5 AML cells were added to 1×10^5 HS-5 cells per well in a final volume of 2 mL in a 24-well plate (Greiner Bio-one, Germany). Cultures were maintained in RPMI-1640 (Sigma-Aldrich, St. Louis, MO) supplemented with 10% fetal calf serum (C. C. Pro, Germany), 2 mM L-glutamine (Sigma-Aldrich), and 40 U/mL penicillin-streptomycin (ThermoFisher Scientific, Waltham, MA) at 37°C in 5% CO_2.

Conditioned medium (CM) was produced by culturing either 2×10^6 HS-5 cells in 20 mL culture medium for 4 days or 5×10^5 AML-MSCs at passage 3 in 20 mL Dulbecco's minimal essential medium supplemented with 30% fetal bovine serum and 1% penicillin, streptomycin, and L-glutamine (all from Sigma-Aldrich) for 6 days. Culture supernatant was harvested and made cell free by centrifugation and filtration. AML cells were cultured at a density of 10^5/mL in fresh culture medium, with or without 50% CM, for 48 hours, unless otherwise stated. In selected experiments CM was depleted from extracellular vesicles by sequential centrifugation at 400*g* for 15 minutes, 2000*g* for 30 minutes, 10 000*g* for 20 minutes, and 100 000*g* for 18 hours with the supernatant of the last centrifugation step.

All inhibitors, chemotherapeutics, cell culture antibodies, recombinant proteins, and compounds used for in vitro cultures are listed in supplemental Table 2.

Statistical analysis

Outliers were determined with the ROUT test. Differences in means were evaluated with parametric (paired or unpaired *t* test or 1-way analysis of variance) or nonparametric (unpaired Mann-Whitney, paired Wilcoxon, or unpaired Kruskal-Wallis) tests based on the number of comparisons (2 or >2) and distribution levels (as determined by Shapiro-Wilk and Kolmogorov-Smirnov). All statistical analyses were performed with GraphPad Prism, version 7 or 8 (GraphPad Software Inc, San Diego, CA) at a significance level of $P < .05$.

Results

Stromal cells promote S100A8/A9 expression in AML in a cell-to-cell, contact-independent manner

First, we purified primary $CD33^+CD34^+CD45^{+/int}$ AML blasts by fluorescence-activated cell sorting from the PB of 6 patients with newly diagnosed AML. These cells were either cultured alone or cocultured with HS-5, a human BM-derived MSC line, for 24 hours. Subsequently, AML blasts were repurified (again) based on CD33, CD34, and CD45 coexpression, and microarray analysis was performed. Both *S100A8* and *S100A9* were among the top 30 significantly upregulated genes upon stromal contact (Figure 1A). In line with previous studies,[13,14] we observed poorer survival in patients with AML with an increased *S100A8* or *S100A9* mRNA expression when performing Kaplan-Meier survival analyses using data generated by TCGA (The Cancer Genome Alas) Research Network (www.cancer.gov/tcga) (Figure 1B). Next, we confirmed our findings by coculturing the AML cell lines OCI-AML and MOLM-13 with HS-5 cells in cell-to-cell contact or with HS-5 CM. In fact, cell-to-cell contact was not essential for the upregulation of either *S100A8* or *S100A9* mRNA and could also be confirmed using primary AML BM-MSC CM (Figure 1C; supplemental Figure 1A). Further analyses revealed the (dose-dependent and reversible) induction of an $S100A8/A9^{high}$ population (on the protein and mRNA levels) among OCI-AML and MOLM-13 cells treated with HS-5 or AML-MSC CM (Figure 1D-E; supplemental Figure 1B-D). The simultaneous upregulation of S100A8 and S100A9 is further suggested by the TCGA AML cohort data displaying a strong correlation between *S100A8* and *S100A9* mRNA expression (Figure 1F). Comparative evaluation of paired AML samples from the PB and BM showed an increased frequency of $S100A8/A9^{high}$ AML blasts within the BM, further corroborating the notion that the BM stroma drives S100A8/A9 levels (Figure 1G). Interestingly, primary $CD33^+CD34^+$ HSCs did not show such induction of S100A8/A9 gene expression or increased formation of $S100A8/A9^{high}$ cells in response to HS-5 CM (supplemental Figure 1E). Because MSCs release bioactive extracellular vesicles (EVs)[25] that shape the BM microenvironment, we depleted EVs in HS-5 CM by ultracentrifugation. However, we did not note any impact of EV depletion on promotion of the $S100A8/A9^{high}$ subset by CM, suggesting that alternative soluble factors were the cause (supplemental Figure 1F).

Stroma cell–derived IL-6 promotes the induction of $S100A8/A9^{high}$ AML cells via Jak/STAT3 signaling

Next, we used a magnetic bead–based multiplex cytokine assay to analyze the HS-5–derived CM. We identified IL-6 as the most abundant of the 25 cytokines tested (Figure 2A). In fact, previous studies have reported production and secretion of IL-6 by MSCs.[26] Treating the AML cell lines with recombinant human IL-6 (rhIL-6) recapitulated the effects of CM in terms of *S100A8/A9* upregulation and enrichment of an $S100A8/A9^{high}$ population (Figure 2B). This result is in line with our observation that expression of IL-6 receptor (IL-6R) correlates significantly with S100A8/A9 in the TCGA AML cohort (supplemental Figure 2A). Blocking IL-6 or IL-6R significantly interfered with the CM-mediated induction of $S100A8/A9^{high}$ cells (Figure 2C). Inflammatory activation (ie, "priming"[27]) of HS-5 cells by interferon-γ and tumor necrosis

Figure 3 (continued) (F) Long-chain fatty acid uptake by AML cell lines (OCI-AML, n = 5; MOLM-13, n = 5) cultured for 48 hours in absence or presence of HS-5 CM was measured by flow cytometry using the fluorescent probe Bodipy FL_{C16} based on the median fluorescence intensity (MdFI). (G) Long-chain fatty acid uptake was analyzed in AML cell lines cultured for 48 hours in the absence or presence of HS-5 CM, with or without ruxolitinib (OCI-AML, n = 2; MOLM-13, n = 3). (H) Oxygen consumption rate (OCR; as a surrogate for oxidative phosphorylation) was determined for MOLM-13 cells (n = 3) cultured for 48 hours in the absence (absence) or presence of HS-5 CM (CM) at baseline and after consecutive injection of SSO and etomoxir, which enabled calculation of the dependence on exogenous (exo) and endogenous (endo) fatty acids for fueling mitochondrial respiration. (I) $S100A8/A9^{hi}$ frequency was analyzed in AML cell lines (OCI-AML, n = 5; MOLM-13, n = 4) cultured for 48 hours in the presence of HS-5 CM, with or without the CD36 inhibitor SSO. Data are expressed as the standard error of the mean. $^*P < .05$; $^{**}P < .01$; $^{***}P < .001$; ns, not significant. DAPI, 4′,6-diamidino-2-phenylindole; FACS, fluorescence-activated cell sorting; qPCR, quantitative real-time polymerase chain reaction.

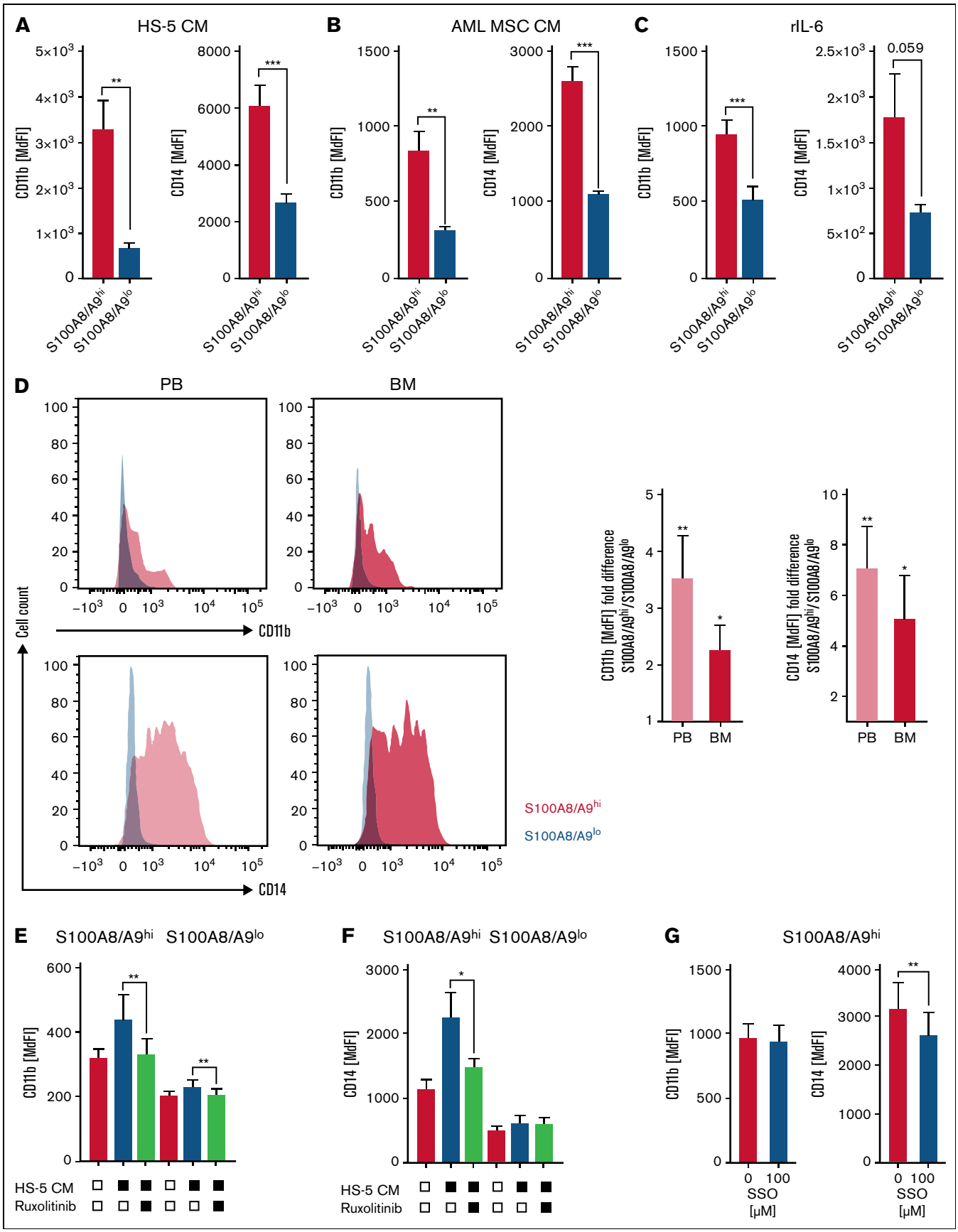

Figure 4.

factor-α, but not by contact with AML cells, boosted *IL-6* expression significantly further, and CM retrieved from primed HS-5 cells displayed a superior ability in driving an S100A8/A9^{high} phenotype (Figure 2D; supplemental Figure 2B). In fact, IL-6 plays a significant role in AML pathogenesis,[28] and *IL-6* expression was higher in MSCs derived from patients with AML compared with healthy control–derived MSCs (Figure 2E).

We identified the STAT3 target genes *PIM1* and *SOCS3* among the top 30 significantly upregulated genes after stromal contact (Figure 1A). We validated the microarray findings by quantitative polymerase chain reaction analysis in AML cell lines treated with CM (Figure 2F). The IL-6/JAK/STAT3 signaling pathway is aberrantly hyperactivated in hematopoietic malignancies and solid tumors.[29] Accordingly, phosphospecific flow cytometry (PhosFlow) staining revealed STAT3 activation in OCI-AML and MOLM-13 cells in the presence of CM, which was most pronounced in S100A8/A9^{high} cells and which could be significantly antagonized by neutralizing IL-6 (Figure 2G-H; supplemental Figure 2C). Simultaneous inhibition of Jak1 and Jak2 (by ruxolitinib) or Jak1 and Jak2 separately also interfered with CM-triggered STAT3 activation (Figure 2I-J). Finally, treatment with both ruxolitinib and C188-9 (a STAT3 inhibitor) attenuated induction of S100A8/9 by CM (Figure 2K-L; supplemental Figure 2D-E), further corroborating the notion that stroma cell–derived IL-6 promotes formation of an S100A8/A9^{high} AML subset in a JAK/STAT3-dependent manner.

S100A8/A9^{high} AML cells are characterized by high CD36 levels and increased uptake of free fatty acids

The fatty acid transporter CD36 has been linked to adverse prognosis, leukemic growth, and chemoresistance in AML.[30-32] The gene and protein expression of CD36 was significantly higher in the S100A8/A9^{high} subset of AML cell lines treated with HS-5– or AML MSC–derived CM or IL-6 (Figure 3A-B; supplemental Figure 3A). This finding was confirmed by ex vivo analysis of primary AML blasts isolated from the PB and BM, showing increased CD36 levels in S100A8/A9^{high} cells and in the TCGA AML cohort exhibiting a strong correlation between CD36 and S100A8/A9 expression (Figure 3C; supplemental Figure 3B). However, reduction of S100A8/A9^{high} cell frequency through siRNA-mediated S100A8/A9 knockdown did not affect CD36 surface levels (supplemental Figure 3C-D). Next, we visualized the subcellular distribution of S100A8 and A9 by confocal microscopy. Apart from the general increase of intracellular protein content, a prominent shift toward the plasma membrane was detected in AML cell lines after treatment with CM (Figure 3D; supplemental Figure 3E). Using proximity ligation assays, we noted that CD36 and S100A8/9 colocalized especially upon treatment with HS-5 CM (Figure 3E; supplemental Figure 3F). In fact, data from a previous study on endothelial cells suggest an interaction between S100A8/A9 and CD36 that, among others, mediates fatty acid uptake.[17] As anticipated, CD36 (together with S100A8/A9) upregulation was paralleled by an enhanced uptake of fatty acids (Figure 3F), which was diminished by both ruxolitinib and S100A8/A9 siRNA (Figure 3G; supplemental Figure 3G). Taken together, those observations suggest that CD36 expression is independent of S100A8/A9, but that activity of fatty acid uptake was fostered by CD36 interacting with S100A8/A9. Metabolic flux analysis revealed a preferential usage of endogenous over exogenous fatty acids to fuel mitochondrial oxidation, which was further increased upon CM treatment (Figure 3H). This finding is similar to the bioenergetic phenotype (including greater mitochondrial mass, supplemental Figure 3H) of chemoresistant AML blasts.[32] Fittingly, we noted an increased storage of fatty acids within lipid droplets that may be subsequently used for energy production (supplemental Figure 3I). Blocking fatty acid transport into cells by sulfo-*N*-succinimidyl oleate (SSO) led to reduced formation of S100A8/A9^{high} cells (Figure 3I), which requires further investigation, as S100A8/A9 heterodimers can bind fatty acids,[33] which in turn (at least in their unsaturated form) reduce protein stability.[34] Interfering with shuttling of fatty acids into the mitochondria, which is required for their oxidation, using etomoxir, had no effect on S100A8/A9 upregulation (supplemental Figure 3K).

S100A8/A9^{high} AML cells display signs of myeloid differentiation

Both S100A8 and S100A9 are regulators of myeloid cell differentiation. S100A8 prevents and S100A9 promotes AML cell differentiation in a TLR4-MAPK/ERK-JNK–dependent manner.[18] In addition, it has been suggested that the ratio between S100A8 and S100A9 determines the differentiation state of myeloid cells. However, both *S100A8* and *S100A9* gene expression correlated significantly with the myeloid differentiation marker CD11b and CD14 within the TCGA AML cohort (supplemental Figure 4A-B). Accordingly, S100A8/A9^{high} AML cells enriched in the presence of HS-5–CM, AML MSC-CM, and rhIL-6 exhibited a significantly increased expression of the myeloid differentiation markers CD11b and CD14 (Figure 4A-C), both of which have been linked to inferior prognosis and higher treatment resistance.[35-37] Likewise, primary S100A8/A9^{high} PB- and BM-derived AML blasts expressed higher CD11b and CD14 cell surface levels compared with their S100A8/A9^{low} counterparts (Figure 4D). Blocking JAK/STAT signaling interferes with the induction of an S100A8/A9^{high} AML population by stromal cells (Figure 2I-L; supplemental Figure 2D-E), and it also prevents upregulation of myeloid differentiation markers (Figure 4E-F). This finding is in accordance with the role of STAT3 as a mediator of myeloid cell differentiation and survival.[38] Blocking fatty acid uptake (by SSO) affected CD14 but not

Figure 4. S100A8/A9^{high} AML cells display signs of myeloid differentiation. (A-C) AML cell lines were analyzed by flow cytometry for the myeloid maturation markers CD11b and CD14 in S100A8/A9^{hi} and S100A8/A9^{lo} cells after 48 hours of culture in the presence of HS-5 CM (A; OCI-AML, n = 5; MOLM-13, n = 5), AML-MSC CM from 6 patients (B; OCI-AML, n = 12; MOLM-13, n = 12, patient ID 11-16; supplemental Table 1), and recombinant human IL-6 (C; OCI-AML, n = 3; MOLM-13, n = 3), based on median fluorescence intensity (MdFI). (D) The myeloid maturation markers CD11b and CD14 were analyzed by flow cytometry in matched-pair (n = 10; patient ID 1-10; supplemental Table 1) PB- and BM-derived S100A8/A9^{hi} and S100A8/A9^{lo} AML blasts, as shown in representative histograms (left) and as summarized by fold change (right; S100A8/A9^{lo} set as 1). (E-F) Surface levels of CD11b and CD14 were analyzed in S100A8/A9^{hi} and S100A8/A9^{lo} (OCI-AML, n = 4; MOLM1,3 n = 4) populations after culture for 48 hours with HS-5 CM in the absence or presence of the pan-Jak inhibitor ruxolitinib, as indicated. (G) Surface levels of CD11b and CD14 were analyzed in S100A8/A9^{hi} cells among the AML cell lines (OCI-AML, n = 5; MOLM-13, n = 5) after 48 hours of culture with HS-5 CM in the absence or presence of the CD36 inhibitor SSO. Data are expressed as the standard error of mean. *$P < .05$; **$P < .01$; ***$P < .001$.

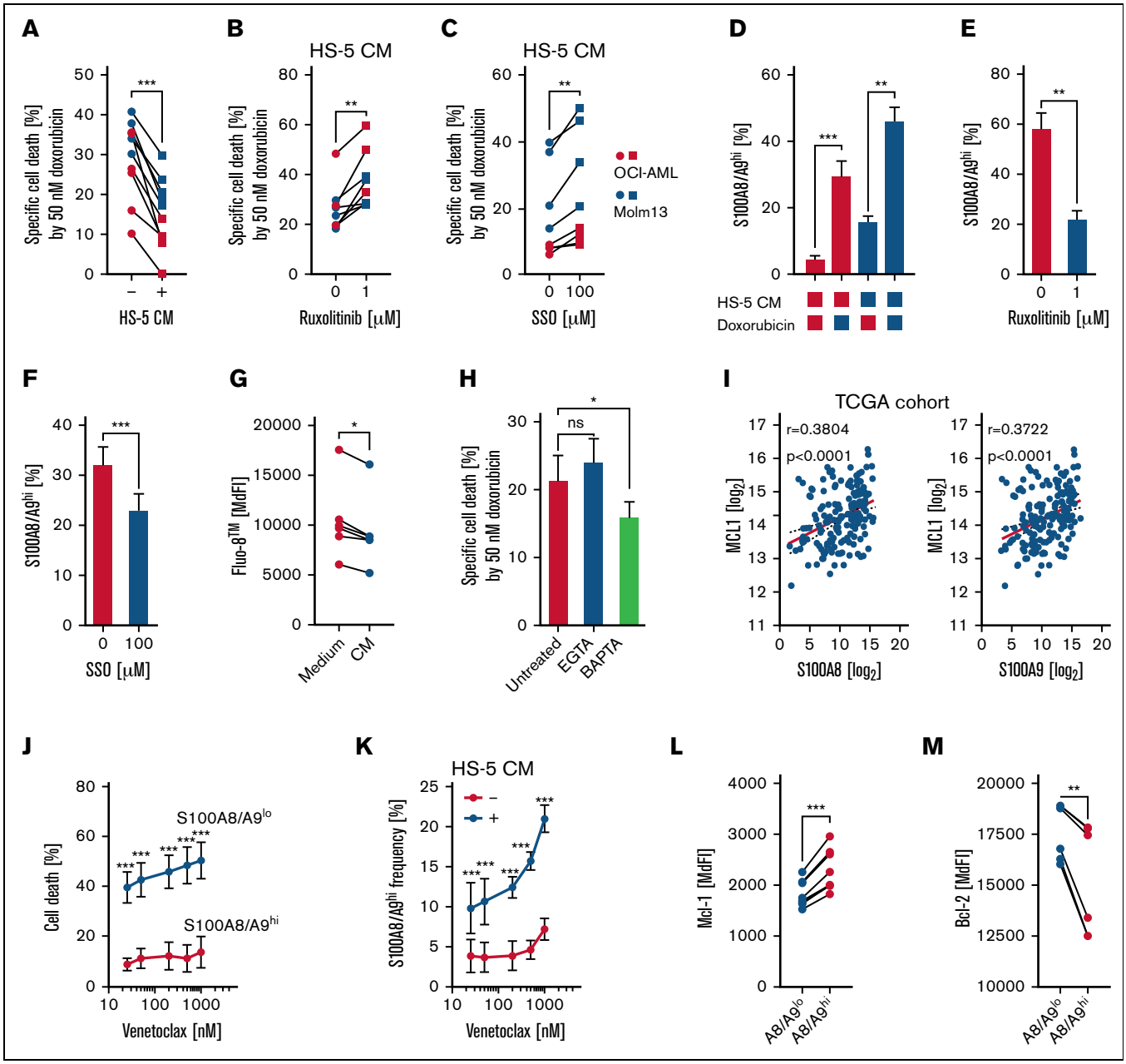

Figure 5. S100A8/A9 expression is associated with enhanced therapeutic resistance. (A) AML cell lines (OCI-AML, n = 5; MOLM-13, n = 5) were incubated for 48 hours in the absence (–, circles) or presence (+, squares) of HS-5 CM and treated with 50 nM doxorubicin for the last 24 hours of culture. Viability was analyzed by annexin-V/7-AAD staining via flow cytometry, and specific cell death by doxorubicin was calculated. (B-C) Similarly, specific cell death by 50 nM doxorubicin of AML cell lines (OCI-AML, n = 3; MOLM-13, n = 2-5) cultured in the presence of HS-5 CM was analyzed in untreated (circles) and treated (squares) samples treated with ruxolitinib (B) or SSO (C). (D) The frequency of S100A8/A9^{hi} OCI-AML (n = 8) and MOLM-13 (n = 11) cells was determined by flow cytometry after 48 hours of culture in the absence and presence of HS-5 CM and upon treatment with 50 nM doxorubicin for the last 24 hours, as indicated. (E-F) Frequency of S100A8/A9^{hi} OCI-AML (n = 3-4) and MOLM-13 (n = 4) cells after culture for 48 hours in the presence of HS-5 CM and for the last 24 hours in the presence of 50 nM doxorubicin was determined by flow cytometry upon treatment with ruxolitinib (E) or SSO (F). (G) Free cytosolic calcium was semiquantified in AML cells (OCI-AML, n = 3; MOLM-13, n = 3) cultured for 48 hours in the absence (medium) or presence (CM) of HS-5 CM with the flow cytometric probe Fluo-8. (H) Specific cell death of AML cells (OCI-AML n = 3; MOLM-13 n = 2) by 50 nM doxorubicin was estimated via annexin-V/7-AAD staining in untreated samples and upon scavenging extracellular (EGTA) and free cytosolic (BAPTA) calcium. (I) Log_2-transformed normalized counts of the *S100A8* and *S100A9* gene expression (from TCGA LAML data set) correlated with the log_2-transformed normalized count of *MCL1* by the Spearman test. (J) Cell death of S100A8/A9^{lo} and of S100A8/A9^{hi} AML cells (OCI-AML, n = 3; MOLM-13, n = 3) cultured for 24 hours in the presence of HS-5 CM was analyzed upon treatment with increasing concentrations of venetoclax by annexin-V/7-AAD staining in flow cytometry. (K) Frequency of S100A8/A9^{hi} AML cells (OCI-AML, n = 2; MOLM-13, n = 2) cultured for 24 hours in the absence or presence of HS-5 CM was determined by flow cytometry after treatment with increasing concentrations of venetoclax . (L-M) Intracellular protein levels of Mcl-1 (L, OCI-AML, n = 4; MOLM-13, n = 4) and Bcl-2 (M, OCI-AML, n = 3; MOLM-13, n = 3) were measured by flow cytometry in S100A8/A9^{lo} and S100A8/A9^{hi} subsets of AML cells cultured for 48 hours in the presence of HS-5 CM. Data are expressed as the standard error of mean. *$P < .05$; **$P < .01$; ***$P < .001$; ns, not significant.

CD11b expression in S100A8/A9^{high} AML cells, whereas blocking fatty acid oxidation (by etomoxir) had no effect on the expression of either molecule (Figure 4G; supplemental Figure 4C-D).

Stromal cell–induced S100A8/A9^{high} AML cell population displays increased resistance to chemotherapy and Bcl-2 targeting

The chemoprotective effect of the stromal niches on AML cells is well established.[39,40] Furthermore, previous studies have suggested that a high expression of the fatty acid translocase CD36, as seen in S100A8/A9^{high} AML cells, is associated with increased chemoresistance.[32,41] First, we validated that AML cells were significantly more resistant to doxorubicin-induced cell death when treated in the presence of HS-5 CM (Figure 5A). Induction of S100A8/A9^{high} AML cells by stroma was efficiently antagonized by blocking JAK/STAT signaling or uptake of fatty acids (Figures 2K-L and 3I). In terms of chemoresistance, we noted a similar effect when treating AML cells in the presence of HS-5 CM with ruxolitinib or SSO (Figure 5B-C). Treatment with doxorubicin led to an enrichment of S100A8/A9^{high} AML cells, most likely more resistant, which was even more pronounced in the presence of HS-5 CM (Figure 5D). This accumulation of S100A8/A9^{high} AML cells was counteracted by interfering with JAK/STAT signaling or fatty acid uptake (Figure 5E-F). S100A8 and S100A9 molecules both contain calcium (Ca^{2+}) binding motifs and can therefore buffer free cytosolic Ca^{2+}, which in turn is essential for chemotherapies to exert their cytotoxic function.[42] Treating AML cell lines with HS-5 CM reduced their intracellular Ca^{2+} levels, whereas chemically depleting intracellular (not extracellular) free Ca^{2+} similarly led to a reduced sensitivity toward doxorubicin (Figure 5G-H), which coincided with a stabilized mitochondrial membrane potential (and an according elevation of reactive oxygen species) reflecting a reduced Ca^{2+} crisis (supplemental Figure 5A). In addition, a recent study demonstrated that elevated S100A8/A9 expression in AML correlates with resistance to Bcl-2 inhibition.[20] However, increased Ca^{2+} binding by S100A8/A9 was most likely insufficient to cause venetoclax resistance. Mcl-1 overexpression can be found in venetoclax-resistant lymphoma and leukemia cell lines[43] and gene expression of the antiapoptotic Mcl-1 correlated positively with S100A8 and S100A9 in the TCGA AML cohort (Figure 5I), whereas Bcl-2 expression showed a negative correlation (supplemental Figure 5B). Next, we validated the earlier report by documenting an increased resilience of S100A8/A9^{high} AML cells in response to venetoclax (Figure 5J). Similar to our observations when treating AML cells with doxorubicin, we found an enrichment of S100A8/A9^{high} cells during treatment with venetoclax, particularly in the presence of HS-5 CM, which at the same time harbored higher Mcl-1 and Bcl-2A1 levels (Figure 5K-L; supplemental Figure 5C-D), as well as lower levels of Bcl-2 (Figure 5M).

Discussion

Therapeutic resistance of AML represents one of the main hurdles in clinical practice. BM stroma promotes survival and therapeutic resistance of AML cells. To date, several underlying mechanisms have been described and include, among others, CXCL-12–driven metabolic reprogramming,[9] upregulation of antiapoptotic proteins,[44] and mitochondrial transfer.[10] Obviously, a better understanding of those processes is a prerequisite for developing novel treatment approaches.

In our present study, BM stroma cells (including AML patient-derived MSCs) promoted (the reversible) induction of the Ca^{2+} binding proteins S100A8 and S100A9, leading to formation of an S100A8/S100A9^{high} subpopulation among AML cells. Consequently, S100A8/S100A9^{high} blasts are found at higher frequencies within the BM niche, compared with the circulation. S100A8/A9 are expressed in myeloid but not lymphoid cells. They represent alarmins and are elevated in inflammatory conditions or malignant entities that can mimic inflammation.[16] In fact, S100A8 and S100A9 overexpression has been reported in genomic cohort analyses of patients with AML.[15,18] High levels of S100A8 and S100A9 correlate with a poor prognosis in adult and pediatric AML,[13,14] and it remains to be elucidated in subsequent studies whether S100A8/S100A9^{high} blasts are of similar prognostic impact.

We identified stromal cell-derived IL-6 as one of the key drivers of S100A8 and S100A9 expression. Serum levels of IL-6 are elevated in patients with AML[45] and may be caused by a nonspecific inflammatory reaction. Furthermore, MSCs, and in particular MSCs, retrieved from patients with AML display enhanced IL-6 production.[46] Signaling through the IL-6R supports proliferation of AML blasts, and using IL-6 blockade has led to prolongation of survival in preclinical AML models.[26,47] Downstream of IL-6, we detected STAT3 activation, which was pharmacologically targetable with different Jak and/or STAT inhibitors and which prevented S100A8/A9 upregulation. In fact, STAT3 binding sites have been located by chromatin immunoprecipitation in the promoter region of S100A8 and S100A9.[48] Previous studies have identified aberrant STAT3 signaling, which is partly ligand dependent, as an important element in AML cell survival and potentially, chemoresistance.[49] However, as inhibition of the IL-6 signaling by blocking antibodies did not have the same magnitude of effect as Jak/STAT inhibition, it is very likely that additional stroma cell-derived factors are involved in the regulation of S100A8 and S100A9 expression in AML.

S100A8/A9 molecules can interact with the fatty acid transporter CD36, thereby enhancing fatty acid uptake.[17] In AML, CD36 promotes growth, chemoresistance, and persistence of leukemic precursors and is linked to an adverse outcome.[21,30,39] Expression of CD36 and colocalization of CD36 with S100A8/A9 was increased upon stromal cross talk. Consequently, we noted a metabolic switch toward the preferential utilization of endogenous and exogenous fatty acids for fueling mitochondrial respiration. This metabolic phenotype resembles chemoresistant AML blasts that are characterized by an overly active CD36-fatty acid oxidation-oxidative phosphorylation axis.[32] Therefore, blocking CD36 with SSO, for example, has attracted considerable attention as a strategy in AML.[31] Formation of S100A8/A9^{high} cells was significantly reduced by SSO, which requires further investigation, as S100A8/A9 heterodimers can bind fatty acids.[33] However, whether S100A8 and S100A9 have a direct effect on fatty acid metabolism remains to be elucidated. In fact, our data indicate that S100A8/A9 induction depends on fatty acids and enhances their usage indirectly via increased CD36 activity.

In terms of myeloid differentiation, S100A8 and S100A9 seem to play contradictory roles. In vitro experiments and preclinical models have revealed that S100A9 promotes differentiation via TLR4, whereas S100A8 blocks differentiation.[18] It has been suggested that the relative ratio between S100A9 and S100A8 finally determines their impact on AML maturation. In this study, S100A8/A9^{high}

AML cells displayed a more mature phenotype, suggesting a dominant role of S100A9. Differentiation, together with S100A8/A9 induction, was triggered by the IL-6-STAT3 pathway. The biological impact of this observation remains unclear, and it could be speculated that pseudomaturation could yield less proliferative, quiescentlike AML cells that are less susceptible to chemotherapeutics that preferentially affect the highly proliferative cell fraction.

As previously published by us and others, stromal cells promote chemoresistance of AML cells, and this effect is successfully antagonized by Jak/STAT and/or CD36 blockade.[30,50] Furthermore, upon treatment with doxorubicin, we documented an enrichment of S100A8/A9^{high} cells among the surviving cell fraction, in line with our aforementioned findings (eg, the metabolic phenotype of S100A8/A9^{high} cells) that imply a superior chemoresistance. Survival of S100A8/A9^{high} cells was diminished when we combined doxorubicin with Jak/STAT or CD36 inhibition. High levels of S100A8/A9 may exert directly antiapoptotic effects by binding free cytosolic Ca^{2+} (most likely released from the endoplasmic reticulum), which is involved in cell death by apoptosis.[51] In addition to conventional chemotherapeutics, S100A8/A9^{high} cells were also less susceptible to the Bcl-2 inhibitor venetoclax.[20] Similarly, this finding may be related to less-available cytosolic Ca^{2+} migrating toward the mitochondria to elicit apoptosis. However, we also found a positive correlation between Mcl-1, which, as an antiapoptotic protein, represents one of the main contributors to venetoclax resistance in AML[52] and S100A8/A9 expression. The AML-specific relationship between Mcl-1 and S100A8/A9 requires further investigation, as S100A8/A9 and Mcl-1 do not correlate in acute lymphoblastic leukemia.[53] Based on previous data, STAT3 signaling may represent an integrating hub for both S100A8/A9 and Mcl-1.[54]

In summary, we demonstrated that BM-resident stromal cells promote a therapy-resistant S100A8/A9^{high} phenotype among AML cells in a contact-independent fashion. Mechanistically, we showed that the induction of S100A8/A9 is mediated by an IL-6/Jak/STAT3 axis and depends on exogenous fatty acids. Therapy resistance is at least partly mediated by the Ca^{2+}-binding nature of S100A8/A9 and their positive correlation with antiapoptotic proteins resulting in diminished apoptosis. Thus, our data append to the complex network of bidirectional cross talk between leukemic blasts and their stromal microenvironment and suggest that targeting induction of S100A8/A9 in AML by different means may represent a promising way to improve treatment efficacy by interfering with BM-derived nurturing signals.

Acknowledgments

The graphical abstract was created using BioRender.com under a personal license held by M.B.

H.B., A.M., and D.M. were supported by the Deutsche Forschungsgemeinschaft (SFB-TRR221 A06 and B12). K.P. was supported by the Interdisziplinäres Zentrum für Klinische Forschung (IZKF) Erlangen.

Authorship

Contribution: M.B. and K.P. performed experiments, analyzed data, and helped writing the manuscript; H.B., M.S., S.V., S.G., B.D., and T.S. performed experiments; A.M. helped designing the study; and D.M. designed the study, analyzed data, and wrote the manuscript.

Conflict-of-interest disclosure: The authors declare no competing financial interests.

ORCID profiles: M.B., 0000-0003-2911-8830; K.P., 0000-0001-8681-2058; M.S., 0000-0002-6923-8776; A.M., 0000-0002-0685-4483.

Correspondence: Dimitrios Mougiakakos, Department of Hematology and Oncology, University Hospital, Otto-von-Guericke University Magdeburg, Leipziger Str 44, 39120 Magdeburg, Germany; email: dimitrios.mougiakakos@med.ovgu.de.

References

1. Estey E, Döhner H. Acute myeloid leukaemia. *Lancet*. 2006;368(9550):1894-1907.
2. Tallman MS, Wang ES, Altman JK, et al; OCN. Acute Myeloid Leukemia, Version 3.2019, NCCN Clinical Practice Guidelines in Oncology. *J Natl Compr Canc Netw*. 2019;17(6):721-749.
3. Méndez-Ferrer S, Bonnet D, Steensma DP, et al. Bone marrow niches in haematological malignancies. *Nat Rev Cancer*. 2020;20(5):285-298.
4. Forte D, García-Fernández M, Sánchez-Aguilera A, et al. Bone Marrow Mesenchymal Stem Cells Support Acute Myeloid Leukemia Bioenergetics and Enhance Antioxidant Defense and Escape from Chemotherapy. *Cell Metab*. 2020;32(5):829-843.e9.
5. Boutin L, Arnautou P, Trignol A, et al. Mesenchymal stromal cells confer chemoresistance to myeloid leukemia blasts through Side Population functionality and ABC transporter activation. *Haematologica*. 2020;105(4):987-998.
6. Garrido SM, Appelbaum FR, Willman CL, Banker DE. Acute myeloid leukemia cells are protected from spontaneous and drug-induced apoptosis by direct contact with a human bone marrow stromal cell line (HS-5). *Exp Hematol*. 2001;29(4):448-457.
7. Samudio I, Harmancey R, Fiegl M, et al. Pharmacologic inhibition of fatty acid oxidation sensitizes human leukemia cells to apoptosis induction. *J Clin Invest*. 2010;120(1):142-156.
8. Cheng J, Li Y, Liu S, et al. CXCL8 derived from mesenchymal stromal cells supports survival and proliferation of acute myeloid leukemia cells through the PI3K/AKT pathway. *FASEB J*. 2019;33(4):4755-4764.
9. Braun M, Qorraj M, Büttner M, et al. CXCL12 promotes glycolytic reprogramming in acute myeloid leukemia cells via the CXCR4/mTOR axis. *Leukemia*. 2016;30(8):1788-1792.
10. Moschoi R, Imbert V, Nebout M, et al. Protective mitochondrial transfer from bone marrow stromal cells to acute myeloid leukemic cells during chemotherapy. *Blood*. 2016;128(2):253-264.

11. Jin L, Hope KJ, Zhai Q, Smadja-Joffe F, Dick JE. Targeting of CD44 eradicates human acute myeloid leukemic stem cells. *Nat Med*. 2006;12(10):1167-1174.
12. Kumar B, Garcia M, Weng L, et al. Acute myeloid leukemia transforms the bone marrow niche into a leukemia-permissive microenvironment through exosome secretion. *Leukemia*. 2018;32(3):575-587.
13. Nicolas E, Ramus C, Berthier S, et al. Expression of S100A8 in leukemic cells predicts poor survival in de novo AML patients. *Leukemia*. 2011;25(1):57-65.
14. Yang XY, Zhang MY, Zhou Q, et al. High expression of S100A8 gene is associated with drug resistance to etoposide and poor prognosis in acute myeloid leukemia through influencing the apoptosis pathway. *OncoTargets Ther*. 2016;9:4887-4899.
15. Ley TJ, Miller C, Ding L, et al; Cancer Genome Atlas Research Network. Genomic and epigenomic landscapes of adult de novo acute myeloid leukemia. *N Engl J Med*. 2013;368(22):2059-2074.
16. Bresnick AR, Weber DJ, Zimmer DB. S100 proteins in cancer. *Nat Rev Cancer*. 2015;15(2):96-109.
17. Kerkhoff C, Sorg C, Tandon NN, Nacken W. Interaction of S100A8/S100A9-arachidonic acid complexes with the scavenger receptor CD36 may facilitate fatty acid uptake by endothelial cells. *Biochemistry*. 2001;40(1):241-248.
18. Laouedj M, Tardif MR, Gil L, et al. S100A9 induces differentiation of acute myeloid leukemia cells through TLR4. *Blood*. 2017;129(14):1980-1990.
19. Leclerc E, Fritz G, Vetter SW, Heizmann CW. Binding of S100 proteins to RAGE: an update. *Biochim Biophys Acta*. 2009;1793(6):993-1007.
20. Karjalainen R, Liu M, Kumar A, et al. Elevated expression of S100A8 and S100A9 correlates with resistance to the BCL-2 inhibitor venetoclax in AML. *Leukemia*. 2019;33(10):2548-2553.
21. Zhu Y, Zhang F, Zhang S, et al. Regulatory mechanism and functional analysis of S100A9 in acute promyelocytic leukemia cells. *Front Med*. 2017;11(1):87-96.
22. Wilhelm BT, Briau M, Austin P, et al. RNA-seq analysis of 2 closely related leukemia clones that differ in their self-renewal capacity. *Blood*. 2011;117(2):e27-e38.
23. Zambetti NA, Ping Z, Chen S, et al. Mesenchymal Inflammation Drives Genotoxic Stress in Hematopoietic Stem Cells and Predicts Disease Evolution in Human Pre-leukemia. *Cell Stem Cell*. 2016;19(5):613-627.
24. Krampera M, Galipeau J, Shi Y, Tarte K, Sensebe L; MSC Committee of the International Society for Cellular Therapy (ISCT). Immunological characterization of multipotent mesenchymal stromal cells–The International Society for Cellular Therapy (ISCT) working proposal. *Cytotherapy*. 2013;15(9):1054-1061.
25. Butler JT, Abdelhamed S, Kurre P. Extracellular vesicles in the hematopoietic microenvironment. *Haematologica*. 2018;103(3):382-394.
26. Zhang TY, Dutta R, Benard B, Zhao F, Yin R, Majeti R. IL-6 blockade reverses bone marrow failure induced by human acute myeloid leukemia. *Sci Transl Med*. 2020;12(538):eaax5104.
27. Mougiakakos D, Jitschin R, Johansson CC, Okita R, Kiessling R, Le Blanc K. The impact of inflammatory licensing on heme oxygenase-1-mediated induction of regulatory T cells by human mesenchymal stem cells. *Blood*. 2011;117(18):4826-4835.
28. Rambaldi A, Torcia M, Bettoni S, et al. Modulation of cell proliferation and cytokine production in acute myeloblastic leukemia by interleukin-1 receptor antagonist and lack of its expression by leukemic cells. *Blood*. 1991;78(12):3248-3253.
29. Johnson DE, O'Keefe RA, Grandis JR. Targeting the IL-6/JAK/STAT3 signalling axis in cancer. *Nat Rev Clin Oncol*. 2018;15(4):234-248.
30. Perea G, Domingo A, Villamor N, et al; CETLAM GroupSpain. Adverse prognostic impact of CD36 and CD2 expression in adult de novo acute myeloid leukemia patients. *Leuk Res*. 2005;29(10):1109-1116.
31. Zhang T, Yang J, Vaikari VP, et al. Apolipoprotein C2 - CD36 Promotes Leukemia Growth and Presents a Targetable Axis in Acute Myeloid Leukemia. *Blood Cancer Discov*. 2020;1(2):198-213.
32. Farge T, Saland E, de Toni F, et al. Chemotherapy-Resistant Human Acute Myeloid Leukemia Cells Are Not Enriched for Leukemic Stem Cells but Require Oxidative Metabolism. *Cancer Discov*. 2017;7(7):716-735.
33. Kerkhoff C, Klempt M, Kaever V, Sorg C. The two calcium-binding proteins, S100A8 and S100A9, are involved in the metabolism of arachidonic acid in human neutrophils. *J Biol Chem*. 1999;274(46):32672-32679.
34. Gheibi N, Ghorbani M, Shariatifar H, Farasat A. Effects of unsaturated fatty acids (Arachidonic/Oleic Acids) on stability and structural properties of Calprotectin using molecular docking and molecular dynamics simulation approach. *PLoS One*. 2020;15(3):e0230780.
35. Graf M, Reif S, Kröll T, Hecht K, Nuessler V, Schmetzer H. Expression of MAC-1 (CD11b) in acute myeloid leukemia (AML) is associated with an unfavorable prognosis. *Am J Hematol*. 2006;81(4):227-235.
36. Choi Y, Lee JH, Kim SD, et al. Prognostic implications of CD14 positivity in acute myeloid leukemia arising from myelodysplastic syndrome. *Int J Hematol*. 2013;97(2):246-255.
37. Nørgaard JM, Olesen LH, Olesen G, et al. FAB M4 and high CD14 surface expression is associated with high cellular resistance to Ara-C and daunorubicin: implications for clinical outcome in acute myeloid leukaemia. *Eur J Haematol*. 2001;67(4):221-229.
38. de Koning JP, Soede-Bobok AA, Ward AC, et al. STAT3-mediated differentiation and survival and of myeloid cells in response to granulocyte colony-stimulating factor: role for the cyclin-dependent kinase inhibitor p27(Kip1). *Oncogene*. 2000;19(29):3290-3298.
39. Ye H, Adane B, Khan N, et al. Leukemic Stem Cells Evade Chemotherapy by Metabolic Adaptation to an Adipose Tissue Niche. *Cell Stem Cell*. 2016;19(1):23-37.

40. Parmar A, Marz S, Rushton S, et al. Stromal niche cells protect early leukemic FLT3-ITD+ progenitor cells against first-generation FLT3 tyrosine kinase inhibitors. *Cancer Res*. 2011;71(13):4696-4706.

41. Sarry JE, Murphy K, Perry R, et al. Human acute myelogenous leukemia stem cells are rare and heterogeneous when assayed in NOD/SCID/IL2Rγc-deficient mice. *J Clin Invest*. 2011;121(1):384-395.

42. Kerkhofs M, Bittremieux M, Morciano G, et al. Emerging molecular mechanisms in chemotherapy: Ca^{2+} signaling at the mitochondria-associated endoplasmic reticulum membranes. *Cell Death Dis*. 2018;9(3):334.

43. Tahir SK, Smith ML, Hessler P, et al. Potential mechanisms of resistance to venetoclax and strategies to circumvent it. *BMC Cancer*. 2017;17(1):399.

44. Konopleva M, Konoplev S, Hu W, Zaritskey AY, Afanasiev BV, Andreeff M. Stromal cells prevent apoptosis of AML cells by up-regulation of anti-apoptotic proteins. *Leukemia*. 2002;16(9):1713-1724.

45. Thomas X, Hirschauer C, Troncy J, et al. Serum interleukin-6 levels in adult acute myelogenous leukemia: relationship with disease characteristics and outcome. *Leuk Lymphoma*. 1997;24(3-4):291-300.

46. Lopes MR, Pereira JK, de Melo Campos P, et al. De novo AML exhibits greater microenvironment dysregulation compared to AML with myelodysplasia-related changes. *Sci Rep*. 2017;7(1):40707.

47. Säily M, Koistinen P, Zheng A, Savolainen ER. Signaling through interleukin-6 receptor supports blast cell proliferation in acute myeloblastic leukemia. *Eur J Haematol*. 1998;61(3):190-196.

48. Rodriguez-Barrueco R, Yu J, Saucedo-Cuevas LP, et al. Inhibition of the autocrine IL-6-JAK2-STAT3-calprotectin axis as targeted therapy for HR-/HER2+ breast cancers. *Genes Dev*. 2015;29(15):1631-1648.

49. Redell MS, Ruiz MJ, Alonzo TA, Gerbing RB, Tweardy DJ. Stat3 signaling in acute myeloid leukemia: ligand-dependent and -independent activation and induction of apoptosis by a novel small-molecule Stat3 inhibitor. *Blood*. 2011;117(21):5701-5709.

50. Karjalainen R, Pemovska T, Popa M, et al. JAK1/2 and BCL2 inhibitors synergize to counteract bone marrow stromal cell-induced protection of AML. *Blood*. 2017;130(6):789-802.

51. Rizzuto R, Pinton P, Ferrari D, et al. Calcium and apoptosis: facts and hypotheses. *Oncogene*. 2003;22(53):8619-8627.

52. Niu X, Zhao J, Ma J, et al. Binding of Released Bim to Mcl-1 is a Mechanism of Intrinsic Resistance to ABT-199 which can be Overcome by Combination with Daunorubicin or Cytarabine in AML Cells. *Clin Cancer Res*. 2016;22(17):4440-4451.

53. Spijkers-Hagelstein JA, Schneider P, Hulleman E, et al. Elevated S100A8/S100A9 expression causes glucocorticoid resistance in MLL-rearranged infant acute lymphoblastic leukemia. *Leukemia*. 2012;26(6):1255-1265.

54. Liu H, Ma Y, Cole SM, et al. Serine phosphorylation of STAT3 is essential for Mcl-1 expression and macrophage survival. *Blood*. 2003;102(1):344-352.